Atm Heterozygosity Cooperates with Loss of *Brca1* to Increase the Severity of Mammary Gland Cancer and Reduce Ductal Branching

T.J. Bowen,[1] Hiroyuki Yakushiji,[1] Cristina Montagna,[3] Sonia Jain,[2] Thomas Ried,[3] and Anthony Wynshaw-Boris[1]

[1]Department of Pediatrics/Medicine and Comprehensive Cancer Center, and [2]Division of Biostatistics and Bioinformatics, Department of Family and Preventive Medicine, University of California-San Diego, La Jolla, California and [3]Genetics Branch, Center for Cancer Research, National Cancer Institute/NIH, Bethesda, Maryland

Abstract

The role of homozygous ataxia telangiectasia mutated (*ATM*) mutations in familial and sporadic forms of cancer is well established, but the contribution of *ATM* heterozygosity to mammary gland and other cancers has been controversial. To test the effect of *Atm* heterozygosity on mammary gland cancer, mice with complete loss of exon 11 of *Brca1* specifically in mammary epithelium (*Brca1*-MG-Δex11) were studied in either *Atm* heterozygous or *Atm* wild-type backgrounds. Targeted deletion of *Brca1* in mammary epithelium resulted in carcinomas and adenocarcinomas of varying histology with long (>9 months) latency. Latency to tumorigenesis was found to be unchanged in the *Brca1*-MG-Δex11;*Atm* heterozygous mice compared with *Brca1*-MG-Δex11;*Atm* wild-type mice. However, the mice displayed variable tumor severity and differences in mammary tissue development. Mammary tumors from *Brca1*-MG-Δex11;*Atm* heterozygous mice were anaplastic and undifferentiated in all 20 tumors tested, whereas tumors from mice that were *Brca1*-MG-Δex11 but wild-type for *Atm* displayed variable histologic profiles, with some anaplastic tumors and other differentiated and less invasive tumor types. Previously reported developmental defects for *Brca1*-deficient mice were also observed in our model with and without *Atm* heterozygosity, but *Brca1*-MG-Δex11;*Atm* heterozygous mice displayed decreased ductal branching during puberty, a phenotype that was not observed in *Brca1*-MG-Δex11;*Atm* wild-type mice. Our results provide evidence that *Atm* heterozygosity influences severity of mammary gland tumors in the *Brca1*-MG-Δex11 tumor-prone mouse and suggest that this mutation leads to a newly characterized developmental defect during glandular maturation. (Cancer Res 2005; 65(19): 8736-46)

Introduction

Breast cancer is the most common nondermatologic cancer diagnosed in humans and the second leading cause of cancer death among women. Tumorigenesis can result from the dysfunction of any of several important oncogenes or tumor suppressors. For example, the tumor suppressor *BRCA1* was one of the first genes to be associated with familial breast cancer susceptibility in humans. Carriers of mutations in *BRCA1* display a much higher (50-85%) lifetime risk of developing breast cancer than noncarriers (1). The pathologic phenotype of tumors associated with *BRCA1*-deficient breast cancer varies widely from nonmalignant adenomas to malignant anaplastic carcinomas that are undifferentiated, aggressive, and highly proliferative.

Mutations in other tumor suppressor genes lead to an increased susceptibility to breast cancer as well. One such gene is ataxia telangiectasia mutated (*ATM*). Homozygous mutation of the *ATM* gene causes the human disease ataxia telangiectasia, a disease characterized by progressive cerebellar ataxia, ocultaneous telangiectasias, immunodeficiency, retarded somatic growth, gonadal dysgenesis, radiosensitivity, and lymphoreticular malignancies (2, 3). Many of these phenotypes are a result of the inability to properly control the cell cycle or respond to DNA damage in the absence of *ATM*. ATM is a critical kinase with many target proteins that are responsible for the maintenance of cell cycle, including known tumor suppressors, such as p53. ATM has also been shown to directly phosphorylate BRCA1 in activation of the cell cycle checkpoints at G_2-M and S-G_2 (4, 5). The loss of *BRCA1* results in cell cycle checkpoint dysfunction, improper DNA damage repair, and genomic instability in the form of translocations, deletions, and duplications (6–8).

Heterozygous carriers of mutations in *ATM* display no overt phenotypes associated with clinical, epidemiologic, and molecular studies of obligate ataxia telangiectasia homozygotes, but some show an increase in susceptibility to cancers, including an increased risk of breast cancer (9–18). This relative risk varies widely among studies from 1.3- to 12.7-fold increase in susceptibility compared with control groups. However, no increased risk levels in the general population have been reported, perhaps because the exact mutations of random carriers are not all known. Most of the studies done have used assays for truncation mutations, and these studies have generally revealed no increase in the susceptibility of female *ATM* carriers relative to noncarriers in populations of women with breast cancer (14, 19–22). By contrast, other studies suggest that there may be a higher prevalence of certain types of *ATM* mutations in breast cancer arising in familial breast cancers but not in nonfamilial sporadic mammary gland cancers (23). For example, a recent study analyzing several different ATM mutations, including five that caused a protein truncation and two causing missense mutations, suggested that *ATM* heterozygosity may cause an 8.5% increased

Note: H. Yakushiji is currently at the Department of Surgery, Taku Hospital, Saga, Japan. C. Montagna is currently at the Department of Pathology, Albert Einstein Medical School, Bronx, New York.

Supplementary data for this article are available at Cancer Research Online (http://cancerres.aacrjournals.org/).

Requests for reprints: Anthony Wynshaw-Boris, Department of Pediatrics/Medicine, University of California-San Diego School of Medicine, 9500 Gilman Drive, Medical Teaching Facility, Room 253, MC 0627, La Jolla, CA 92093-0627. Phone: 858-822-3400; Fax: 858-822-3409; E-mail: awynshawboris@ucsd.edu.

doi:10.1158/0008-5472.CAN-05-1598

risk in families with hereditary breast and ovarian cancers (24). These same mutations were analyzed in the general population and no increased risk for breast cancer was found, suggesting that the effects may be limited to familial cases (25). It has also been shown that a low concentration of *ATM* transcripts is highly correlated with breast carcinomas, moderate expression with benign lesions, and expression at highest levels in normal mammary tissue (26, 27). Finally, a mouse model of an *Atm* heterozygous missense mutant (ΔSRI) that recapitulates the increased susceptibility to cancers, including mammary tumors, has also been generated (28). The data all suggest that *ATM* loss may play some role in the initiation, progression, and/or maintenance of breast tumors when a familial breast cancer gene, such as *BRCA1*, is also absent, although this has not been specifically addressed in human studies.

The mouse provides an alternative way to address the relationship of *Atm* and *Brca1* in mammary gland cancer. Both genes have been knocked out in mice and allow the controlled manipulation of these genes to determine if there is a synergistic effect when both are disrupted. *Brca1*-deficienct mice display an early embryonic lethal phenotype (29–35). Because of this, conditional knockout mice have been generated that allow the spatial and temporal deletion of exon 11 of *Brca1* (35). When Cre-recombinase was expressed from either the mouse mammary tumor virus long terminal repeat promoter (MMTV-LTR) or the whey acidic protein promoter, *Brca1* was deleted specifically in mammary epithelium (35). These mice displayed variable types of mammary carcinomas, commonly ductal and lobular carcinomas as well as more rare cases of squamous carcinomas, medullary carcinomas, and anaplastic carcinomas, all of which are found in human familial breast cancers (36, 37). Mouse models of ataxia telangiectasia have also been generated and they recapitulate the lymphoma tumor phenotype seen in humans with the disease (38, 39). *Atm*-deficient mice develop lymphomas between 2 and 4 months of age (38, 39). These tumors display the characteristic genomic aberrations and cell cycle defects that are found in the human disease and these defects are very similar to those also seen in *Brca1*-deficient mammary gland tumors (34, 40, 41). Cancers from both *Atm* and *Brca1* knockouts display several obvious similarities, including diminished DNA damage response, cell cycle defects, and extensive genomic rearrangements.

These studies together suggest that there may be a link between *Atm* haploinsufficiency and loss of *Brca1* that can be effectively investigated using the mouse as a model. We hypothesized that *Atm* heterozygosity might exacerbate the cancer phenotype associated with *Brca1* loss in mammary. Therefore, we produced mice with complete loss of exon 11 of *Brca1* in mammary epithelium that were either wild-type or heterozygous for an *Atm*-null allele. Latency to tumorigenesis and tumor types as well as mammary gland development were studied. We found that *Atm* haploinsufficiency resulted in absence of differentiated tumor types and increased invasiveness as well as reduced ductal branching in virgin mice, supporting a role for *Atm* in mammary gland tumorigenesis and development.

Materials and Methods

Mice, genotyping, and tumor latency. *Brca1* conditional knockout mice (35), with the MMTV-Cre A1 line (35, 42, 43), were mated with *Atm* heterozygous mice (38) and back-crossed to obtain $Atm^{+/-}$;*Brca1*-MG-Δex11, $Atm^{+/+}$;*Brca1*-MG-Δex11, and $Atm^{+/-}$;$Brca1^{Co/Co}$ mice as a control for loss of *Brca1* in the mammary gland. The *Atm*, *Brca1*, and MMTV-Cre status of the mice, mammary tumors, and cell lines was determined by PCR using *Atm*, *Brca1*, and MMTV-Cre probes as described previously (35, 38, 40, 41). Animals in all groups were checked weekly for tumors. At the onset of tumors, the mice were noted and tumors were harvested at no more than 1.5 cm in diameter. Complete autopsies were done on all mice that developed tumors. Survival time of mice was used to generate Kaplan-Meier survival curves that were compared using log-rank (Mantel-Cox) test.

Western blot and quantitative real-time PCR analysis. Frozen tumor tissue was homogenized and lysed in Triple Lysis Buffer (50 mmol/L Tris, 1 mmol/L EDTA, 0.5% Tween) with proteinase inhibitors added. A Bradford assay was used to quantify protein. For Western blot analysis, protein (100 μg) was subjected to PAGE in a 3% to 8% Tris-acetate gel and transferred to Immobilon membranes. Western analysis was done using standard procedures. Antibodies to c-Myc, estrogen receptor (ER)-α, erbB2, cyclin D1, cyclin A, cdc2, and p27 were purchased from Santa Cruz Biotechnology (Santa Cruz, CA) and BRCA1 was purchased from Oncogene Research Products (La Jolla, CA).

RNA was prepared from 16 $Atm^{+/+}$;*Brca1*-MG-Δex11 and 16 $Atm^{+/-}$;*Brca1*-MG-Δex11 tumors and 2 $Atm^{-/-}$ mouse embryonic fibroblast cell lines. Superscript (Invitrogen, Carlsbad, CA) enzyme was used for reverse transcription and random hexamers were used as primers. Quantitative real-time PCR assays were done at the Center for AIDS Research Genomics Core (Veteran's Medical Research Foundation, La Jolla, CA). Forward and reverse primers were created for *Atm* quantitative PCR (forward primer CCAGCTTTTGATCGAGATACCA and reverse primer CCCAGCCTACGTC-TATTTTCCT). Primers for glyceraldehyde-3-phosphate dehydrogenase (GAPDH) were used for normalization (GAPDH-forward CCACCCATGG-CAAATTCC and GAPDH-reverse TGGGATTTCCATTGATGACAAG). Platinum SYBR Green qPCR SuperMix UDG (Invitrogen) was used for the amplification and detection of cDNA in quantitative real-time PCR.

Immunohistochemistry, histology, and terminal deoxynucleotidyl transferase–mediated dUTP nick end labeling assays. Samples were fixed in 4% paraformaldehyde and stored at 4°C. Sections (5 μm) were cut for tumor and mammary tissues and mounted on slides. Tumor and mammary sections, mammary tissue whole mounts, and H&E staining were done by University of California-San Diego (UCSD) Cancer Center Histology and Immunohistochemistry Shared Resource (La Jolla, CA) using standard procedures. For immunohistochemistry, samples were also prepared using standard protocol. Antibodies against smooth muscle actin, cytokeratin 5, and vimentin were used for tumor typing (Santa Cruz Biotechnology). Terminal deoxynucleotidyl transferase–mediated dUTP nick end labeling (TUNEL) assay was carried out on 5-μm mammary gland cross-sections using standard protocol.

Spectral karyotyping and comparative genome hybridization. Tumor metaphases were fixed from passage 0 or 1 tumor cells cultured in DMEM/F-12 supplemented with 5% fetal bovine serum, epidermal growth factor, and insulin. Metaphases were generated from four cell lines representing two $Atm^{+/+}$;*Brca1*-MG-Δex11 and two $Atm^{+/-}$;*Brca1*-MG-Δex11 anaplastic tumors. Spectral karyotyping and comparative genome hybridization (CGH) were done as described previously (41). Clones were labeled by nick translation and hybridized to tumor metaphase chromosomes according to standard procedures. Images were acquired using a DMRXA microscope (Leica, Wetzlar, Germany) connected to a Sensys charge-coupled device camera (Roper Scientific, Tucson, AZ) using Q-FISH software (Leica Microsystems, Cambridge, United Kingdom).

Expression analysis. Total RNA was isolated from six anaplastic carcinomas using Trizol reagent and standard protocol (three $Atm^{+/-}$; *Brca1*-MG-Δex11 tumors and three $Atm^{+/+}$;*Brca1*-MG-Δex11 tumors). Total RNA was also isolated from two less aggressive tumors (one ductal carcinoma and one papillary carcinoma) from two mice from the $Atm^{+/-}$;$Brca1^{Co/Co}$;*MMTV-Cre*− control group. These were the only tumors that developed from this cohort. The RNA was checked for integrity and hybridized to Affymetrix U74Av2 probe arrays according to the manufacturer's protocol by the UCSD Cancer Center Microarray Shared Resource (VA Gene Chip Core).

Analysis was done using both dChip and Robust Multichip Average (RMA) analyses for hierarchical clustering and scatter plot analysis using

the Bioconductor: open source software for bioinformatics.[4] RMA preprocessing consisted of three steps: background adjustment, normalization, and summarization. The RMA background noise adjustment corrected for processing effects and cross-hybridization. We implemented normalization to reduce the nonbiological variation across the chips in an experiment, including technical variability, which is related to the experimental procedure of the assay. RMA used the quantile normalization technique to adjust the gene expression intensities such that the distributions of the probe intensities are the same across all chips. The last step, summarization, calculated a single gene expression value by mathematically combining the probe intensities from each probe set. RMA employs the robust multichip linear model fitted on a log scale. Note that the RMA-transformed gene expression intensity calculations were based only on perfect match values from each probe set, because the inclusion of the mismatch probes is believed to contaminate true expression. Aside from measuring nonspecific hybridization, mismatch probes also measure true expression, so valuable signal may be lost when incorporating mismatch probes in expression calculations. By contrast, dChip relied on "invariant set nonlinear normalization" to reduce the variability for low expression estimates and account for both nonlinear and nonbiological effects. We again analyzed perfect match probes only without correction for mismatch hybridization. Note that background adjustment was not conducted here.

The second stage of analysis employed unsupervised clustering to determine if the two classes of tumors could be recovered from the data. Clustering was separately done after preprocessing by RMA and dChip. Dendograms of expression patterns and samples were computed via hierarchical clustering using average linkage as the between-cluster distance criteria and Euclidean distance as the similarity measure.

Results

Generation of *Atm* heterozygous, *Brca1* conditional knockout mice. To analyze the possible effects that *Atm* heterozygosity may have during tumorigenesis in mammary tissue that lacks intact *Brca1*, mice carrying mutations for either *Brca1* or *Atm* were mated to generate a compound genotype. Mice bearing two conditional *Brca1* alleles (called $Brca1^{Co/Co}$) as well as a Cre-recombinase transgene under control of the promoter of the MMTV-LTR gene (MMTV-LTR A1) as described previously were used in the study (called *MMTV-Cre+*; refs. 42, 43). MMTV-Cre deletes exon 11 of the *Brca1* gene in mammary epithelium causing a *Brca1* mutation (35, 40, 41). These mice (called *Brca1*-MG-Δex11) were crossed with mice heterozygous for mutant *Atm* (called $Atm^{+/-}$; ref. 38). After crossing mice to generate either $Atm^{+/-}$;*Brca1*-MG-Δex11 or $Atm^{+/-}$;$Brca1^{Co/Co}$;*MMTV-Cre−* genotypes, all were in a mixed background. Littermate controls were generated for the study having one of three genotypes. $Atm^{+/-}$;*Brca1*-MG-Δex11 and $Atm^{+/+}$;*Brca1*-MG-Δex11 mice were the experimental groups and would express *Brca1* exon 11 mutant alleles in the mammary epithelium. $Atm^{+/-}$;$Brca1^{Co/Co}$;*MMTV-Cre−* mice were used as a control group.

***Atm* haploinsufficiency does not alter latency to tumorigenesis in *Brca1* mutant mice.** Females of all three groups were continuously mated to maintain high levels of MMTV-Cre and monitored for mammary gland tumor formation. No mammary tumors were detected between 0 and 9 months of age in any cohort. However, between 9 and 26 months, 43% of $Atm^{+/-}$;*Brca1*-MG-Δex11 (20 of 46) and 56% of $Atm^{+/+}$;*Brca1*-MG-Δex11 (28 of 50) mice developed mammary tumors. This was slightly higher than previous reports of 25% to 30% penetrance (35, 40). Kaplan-Meier analysis of survival indicated a significant difference in overall survival between the control $Atm^{+/-}$;$Brca1^{Co/Co}$;*MMTV-Cre−* group and the two *Brca1*-MG-Δex11 groups (Fig. 1*A*). The mice that did not express the MMTV-Cre transgene retained both alleles of *Brca1* and would display normal *Brca1* expression. However, there was no difference in the latency to tumorigenesis between $Atm^{+/-}$;*Brca1*-MG-Δex11 and $Atm^{+/+}$;*Brca1*-MG-Δex11 mice ($P > 0.56$; Fig. 1*B*). Two control mice that were $Atm^{+/-}$;$Brca1^{Co/Co}$;*MMTV-Cre−* (2 of 40) developed mammary tumors at 18 months of age.

To determine whether there was loss of heterozygosity (LOH) of *Atm* in $Atm^{+/-}$ tumors, both standard PCR (done with DNA from both tails and tumors of corresponding animals) and quantitative real-time PCR (done with total RNA isolated from frozen tumor tissue) were done. All $Atm^{+/-}$ tumors retained both *Atm* mutant and wild-type alleles, whereas all *Atm* wild-type tumors retained wild-type alleles (Fig. 1*C* and *D*). All tumors were analyzed for loss of BRCA1 protein via Western blot, which revealed normal levels of expression in $Atm^{+/-}$ and $Atm^{-/-}$ mouse embryonic fibroblast control cell lines (Fig. 1*E*) and decreased levels of BRCA1 from tumors that developed in the $Atm^{+/+}$;*Brca1*-MG-Δex11 or $Atm^{+/-}$;*Brca1*-MG-Δex11 mice. Quantitative real-time PCR indicated that the amount of *Atm* RNA from $Atm^{+/-}$;*Brca1*-MG-Δex11 tumors was approximately half the level of RNA from $Atm^{+/+}$;*Brca1*-MG-Δex11 animals (Fig. 1*F*). These findings show that the *Atm* alleles remain intact in tumors from the $Atm^{+/-}$;*Brca1*-MG-Δex11 mice and do not undergo LOH and that any phenotypic differences may be the result of *Atm* haploinsufficiency.

***Atm* haploinsufficiency alters tumor severity in *Brca1* mutant mammary tissue.** Histologic analysis revealed that the tumors from $Atm^{+/+}$;*Brca1*-MG-Δex11 mice were variable in type as reported previously for mouse mammary tumors of *Brca1*-deficient tissues (40). These tumors varied in type from well differentiated to undifferentiated (Fig. 2*A-E*) and included adenocarcinomas with some squamous carcinomas, fibroadenomas, fibrillary carcinomas, ductal carcinomas, papillary carcinomas, and spindle cell and anaplastic carcinomas. These tumor histologic types observed are representative of the human breast cancers seen in familial cancer and cancers associated with BRCA1 mutations (36, 37). Interestingly, when the heterozygous $Atm^{+/-}$;*Brca1*-MG-Δex11 tumors were analyzed histologically, we found that all 20 tumors were anaplastic, invasive carcinomas, with a completely undifferentiated appearance (Fig. 2*F*), whereas none showed the less invasive, encapsulated, ductal, or squamous features that are associated with more differentiated tumor types, such as many of those seen in the $Atm^{+/+}$;*Brca1*-MG-Δex11 (Fig. 2*A-D*). The anaplastic tumors of both genotypes were consistent in appearance and rate of growth.

Tumor cell lines were established from several anaplastic tumors of both $Atm^{+/+}$ and $Atm^{+/-}$ genotypes and analyzed with immunohistochemical markers for cell lineage, proliferation, and common mammary gland tumor markers. We compared the expression levels of some typical markers for *Brca1*-deficient tumors with tumors from mice expressing the MMTV-polyomavirus middle T antigen used previously as a positive control for some typically expressed markers in the *Brca1*-deficient tumors (44). Both $Atm^{+/-}$;*Brca1*-MG-Δex11 and $Atm^{+/+}$;*Brca1*-MG-Δex11 tumor cells expressed the markers cytokeratin 5, cytokeratin 8, and vimentin, indicating that they were of ductal origin as expected (data not shown).

It has been shown that the overexpression of cell cycle and oncogenic proteins, such as erbB2, c-Myc, and cyclin D1, occur in tumors from mice with loss of exon 11 of *Brca1* (41, 45, 46). To determine if the $Atm^{+/-}$;*Brca1*-MG-Δex11 and $Atm^{+/+}$;*Brca1*-MG-Δex11 mice were similar or different in the regulation of these

[4] http://www.bioconductor.org.

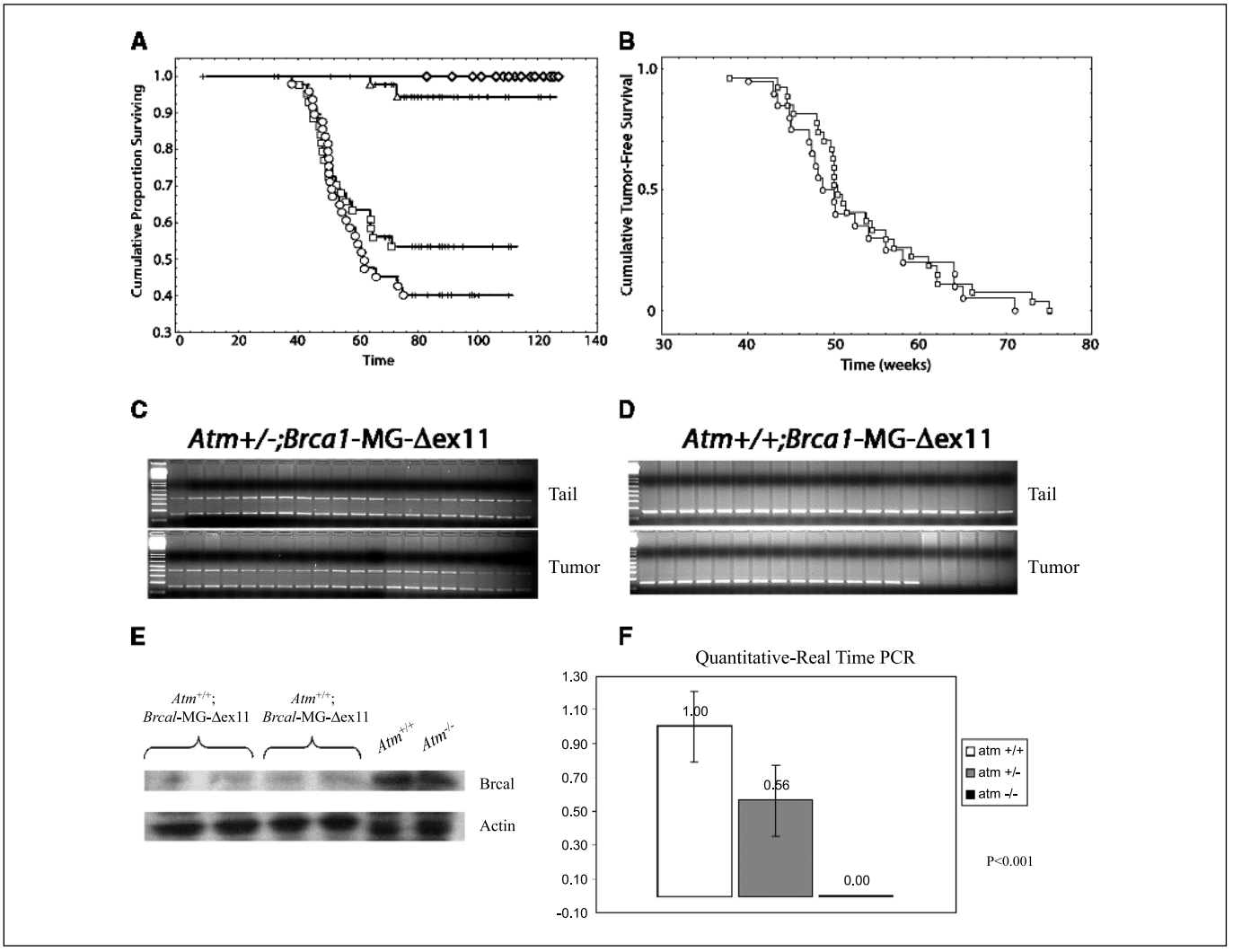

Figure 1. Survival analysis of *Atm*$^{+/+}$;*Brca1*$^{Co/Co}$;*MMTV-Cre*−, *Atm*$^{+/-}$;*Brca1*$^{Co/Co}$;*MMTV-Cre*−, *Atm*$^{+/-}$;*Brca1*-MG-Δex11, and *Atm*$^{+/+}$;*Brca1*-MG-Δex11 mice and tumor analysis. *A,* Kaplan-Meier analysis showed that *Atm*$^{+/+}$;*Brca1*$^{Co/Co}$;*MMTV-Cre*− (◇), *Atm*$^{+/-}$;*Brca1*$^{Co/Co}$;*MMTV-Cre*− (△) survived much longer and developed fewer tumors than either *Atm*$^{+/-}$;*Brca1*-MG-Δex11 (□) or *Atm*$^{+/+}$;*Brca1*-MG-Δex11 mice (○). *B,* Kaplan-Meier analysis was done as in (*A*), but for latency to tumorigenesis, removing animals that died from causes other than tumors. *C* and *D,* PCR genotyping for *Atm* of *Atm*$^{+/+}$;*Brca1*-MG-Δex11 and *Atm*$^{+/-}$;*Brca1*-MG-Δex11 mice and the resulting tumors. *E,* Western blot analysis of *Brca1* levels in *Atm*$^{+/+}$;*Brca1*-MG-Δex11 and *Atm*$^{+/-}$;*Brca1*-MG-Δex11 mice. *F,* quantitative real-time PCR of *Atm* levels from *Atm*$^{+/-}$;*Brca1*-MG-Δex11 mice, *Atm*$^{+/+}$;*Brca1*-MG-Δex11 tumors, and *Atm*$^{-/-}$ mouse embryonic fibroblast controls.

proteins, we did Western blot analysis on several tumors (15 *Atm*$^{+/-}$;*Brca1*-MG-Δex11 and 15 *Atm*$^{+/+}$;*Brca1*-MG-Δex11 mice). We found that cyclin D1, cdc2, c-Myc, and erbB2 were all overexpressed in *Brca1* exon 11–deficient mammary tumors of either *Atm* genotype compared with normal mammary tissues (Fig. 3). Previous studies suggest that cyclin A was not up-regulated in asynchronous tumor cells grown in culture (40, 45). No tumors displayed expression of cyclin A, whereas normal mammary tissues did, supporting previous finding (40). Protein levels of p27 were slightly up-regulated in these tumors compared with control samples, supporting aberrant cell cycle regulation. No obvious differences were observed between differentiated and undifferentiated tumors from *Atm*$^{+/+}$ or undifferentiated tumors from *Atm*$^{+/-}$ mice. This suggests that *Atm* heterozygosity does not affect protein marker expression levels seen in other *Brca1*-deficient mammary tumor models. Tumors were evaluated for ER expression because it was found that tumors resulting from *Brca1* deficiency fall into a basal subtype and are typically ER negative (47). We found that all *Atm*$^{+/-}$;*Brca1*-MG-Δex11 mice and 13 of 15 *Atm*$^{+/+}$;*Brca1*-MG-Δex11 mice were ER negative (Fig. 3).

Similar genomic abnormalities between *Atm*$^{+/-}$ and *Atm* wild-type mammary tumors in a *Brca1* exon 11–deficient background. Previous studies showed that loss of *Brca1* exon 11 in the mammary gland resulted in tumors with genomic instability, including aneuploidy, chromosomal translocations, and loss and gain of chromosomal regions (40, 41). To address whether genomic differences were occurring between the aggressive tumors of each genotype, spectral karyotyping and CGH were used to analyze anaplastic carcinomas of both *Atm*$^{+/-}$;*Brca1*-MG-Δex11 and *Atm*$^{+/+}$;*Brca1*-MG-Δex11 genotypes. Primary cell lines were established from four anaplastic tumors, two from each genotype. Attempts to culture cell lines from the less aggressive tumors were not successful. Spectral karyotyping analysis was done on four different cell lines that were derived from primary tumors at passage 0 or 1. All four tumors revealed numerous chromosomal aberrations, including complex rearrangements,

duplications, and deletions (Fig. 4*A*). Complex rearrangements were observed involving chromosomes 1, 10, and 17. Duplications, deletions, and translocations were commonly observed on most chromosomes. However, quantification of the number of aberrations per chromosome revealed no difference between *Atm*$^{+/-}$;*Brca1*-MG-Δex11 and *Atm*$^{+/+}$;*Brca1*-MG-Δex11 genotypes (Fig. 4*B*).

CGH was used to analyze the loss or gain of chromosomal regions in these four tumor lines and revealed gains and losses representing regions on nearly all chromosomes (Fig. 4*C*). Amplification of the distal end of chromosome 11, and the amplification of the proximal end of chromosome 15, including band 15D, which contains the c-Myc oncogene, was observed. Only two major distinctions were noted between the two genotypes of tumors via CGH. The distal region of chromosome 4 showed loss in both *Atm*$^{+/-}$;*Brca1*-MG-Δex11 tumors, whereas there was no loss in the *Atm*$^{+/+}$;*Brca1*-MG-Δex11 tumors, indicating the loss of the INK4A/ARF locus (Fig. 4*C*). In addition, there was a gain of the proximal portion of the X chromosome in all four tumors as well as the distal end of the X chromosome for the *Atm* wild-type tumors, whereas the *Atm*$^{+/-}$ tumors showed no amplification or deletion of the distal region (Fig. 4*C*).

Expression analysis reveals tumor similarity between genotypes. To determine if there were expression differences based on genotype or tumor type, microarray analysis was done on six anaplastic carcinomas (three tumors from each genotype) and two more highly differentiated tumors from *Atm*$^{+/+}$;*Brca1*-MG-Δex11 mice. RNA was isolated from frozen tissue and hybridized to Affymetrix oligonucleotide arrays containing ~12,000 genes. The resulting expression profiles for each tumor were normalized and compared with both dChip and RMA analyses. Hierarchical clustering resulted in the two noninvasive carcinomas being grouped separately, whereas all of the anaplastic carcinomas clustered more closely. The separate clustering of the noninvasive and invasive carcinomas was expected based on their differences in histologic degree of differentiation. The anaplastic carcinomas could not be differentiated based on *Atm* genotype, though, suggesting that these tumors were very similar in expression and that genotype differences have no obvious effect on global gene expression (Fig. 5). Of the 12,000 genes that were analyzed in this

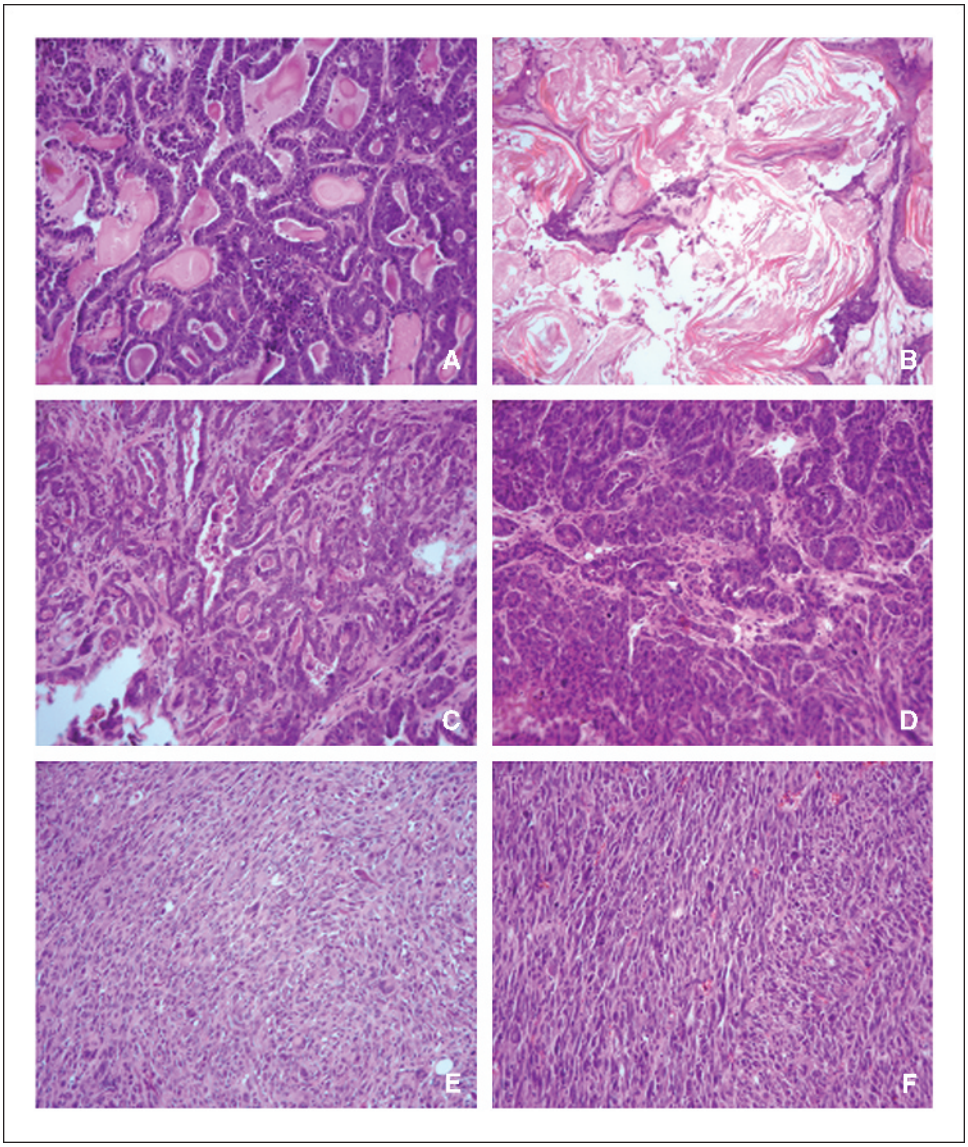

Figure 2. Histologic analysis of tumors from both *Atm*$^{+/+}$;*Brca1*-MG-Δex11 and *Atm*$^{+/-}$;*Brca1*-MG-Δex11 tumors reveals differences. *Atm*$^{+/+}$;*Brca1*-MG-Δex11 tumors (*A*-*E*) were variable in type and level of differentiation. Examples of types of tumors occurring were secretory carcinomas (*A*), squamous carcinomas (*B*), papillary carcinomas (*C*), ductal carcinomas (*D*), and anaplastic carcinomas (*E*), all of varying degrees of differentiation. *Atm*$^{+/-}$;*Brca1*-MG-Δex11 tumors were all undifferentiated, invasive, anaplastic carcinomas (*F*). The anaplastic carcinomas from the two different genotypes were indistinguishable histologically (*E* and *F*).

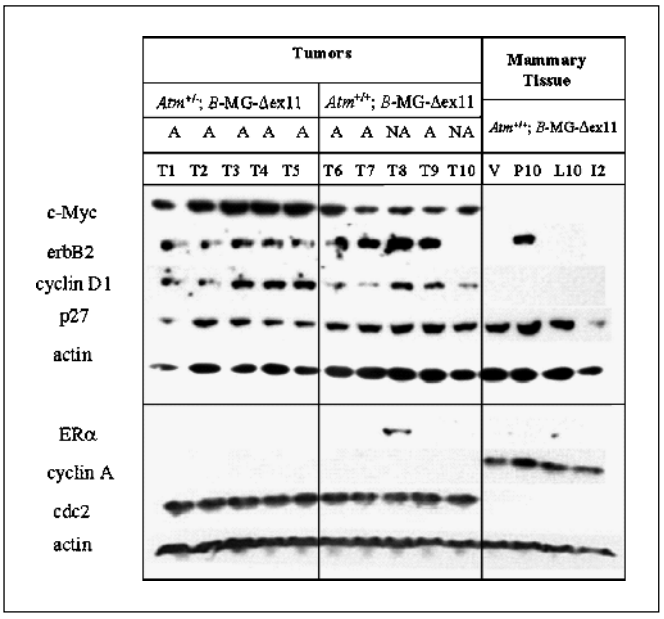

Figure 3. Western blot analysis of c-Myc, erbB2, cyclin D1, p27, ER-α, cyclin A, and cdc2 in mammary tumor samples of *Atm*$^{+/+}$;*Brca1*-MG-Δex11 (*T1-T5*) and *Atm*$^{+/-}$;*Brca1*-MG-Δex11 (*T6-T10*) mice as well as normal mammary tissues from virgin (*V*), pregnancy day 10 (*P10*), lactation day 10 (*L10*), and involution day 2 (*I2*). *A,* anaplastic; *NA,* nonanaplastic.

expression panel, only 16 were consistently expressed at a significantly different level in the *Atm*$^{+/+}$;*Brca1*-MG-Δex11 anaplastic carcinomas compared with the *Atm*$^{+/-}$;*Brca1*-MG-Δex11 carcinomas with the RMA analysis method. Thirteen genes were differentially expressed using the dChip method for the same group of genes. Of these genes, only 5 were considered significant by both methods of analysis. These genes include two Riken clones, DEAD box polypeptide 6, T-box 15, and protein kinase, lysine deficient 1 (Supplementary Table S1). The low number of genes identified by both methods again suggests that the anaplastic tumors were very similar independent of *Atm* genotype.

***Atm* haploinsufficiency leads to decreased ductal branching during early mammary development.** *Brca1* conditional knockout mice display defects in mammary gland development (35), including incomplete penetrance of the mammary fat pad and increased levels of apoptosis. These observations as well as the more anaplastic tumor phenotype in *Atm*$^{+/-}$;*Brca1*-MG-Δex11 mice lead us to analyze mammary development to ascertain if there are any differences between genotypes. Glandular development was analyzed using whole mounts of mammary glands from mice of each genotype at several stages of development, 7-week-old virgins, pregnancy days 8.5 and 16.5, lactation days 1 and 10, and involution. We observed the expected developmental defects in *Brca1* conditional knockout mice during pregnancy and lactation, such as the incomplete penetrance of the mammary fat pad and increased levels of apoptosis (data not shown). However, when analyzing 7-week-old virgin glands for ductal branching, we found that *Atm*$^{+/-}$;*Brca1*-MG-Δex11 glands (Fig. 6*C*) displayed significantly fewer bifurcations than either control (Fig. 6*A*) or *Atm*$^{+/+}$;*Brca1*-MG-Δex11 glands ($P = 0.0004$; Fig. 6*B*, quantitated in Fig. 6*D*). Glands analyzed at early pregnancy showed no differences, whereas those analyzed at late pregnancy displayed slightly decreased density in glandular structure but were not significantly different ($P = 0.158$; data not shown). There were no differences between the two experimental groups during lactation or involution stages. Differences in infiltration into the adipose tissue were observed between the experimental groups and the wild-type *Brca1* control groups as reported previously (35). These defects include failure to completely infiltrate the fat tissue during pregnancy and some underdeveloped areas during lactation (data not shown).

Matched cross-sections from both 7-week-old virgin and midpregnancy mammary glands were analyzed for apoptosis and proliferation. TUNEL assays were done on sections from each of the two experimental groups and a control group to analyze the level of apoptosis in virgin female mammary glands. Similar numbers of apoptotic cells were found in all three groups ($n = 10$; $P = 0.463$; data not shown). The proliferation marker Ki-67 was done on serial sections matching those used in the TUNEL assay to determine the level of proliferation, and similar levels of proliferation were found in both control and experimental groups ($n = 10$; $P = 0.671$; data not shown). Five-week-old virgin mammary glands from *Atm*$^{+/-}$;*Brca1*-MG-Δex11 mice were also sectioned and compared with age-matched wild-type glands to analyze terminal end bud (TEB) morphology and marker expression. *Atm*$^{+/-}$;*Brca1*-MG-Δex11 TEBs appeared normal in morphology with no signs of defective organization in the cap cell layer or prelumenal cells (Fig. 6*E-G*) compared with wild-type controls (Fig. 6*H-J*). Expression of E-cadherin, which adheres prelumenal and lumenal epithelial cells, appears normal as does the expression of P-cadherin, which binds myoepithelial layers (data not shown).

Discussion

We have analyzed the role that *Atm* heterozygosity plays in tumorigenesis and development in *Brca1*-null murine mammary tissue. Previous human studies revealed contradictory evidence for the role that *Atm* heterozygosity may play in tumorigenesis. Early studies based on obligate carrier status in families with affected ataxia telangiectasia individuals suggested that the loss of one allele of *Atm* might result in an increased susceptibility to cancer (10, 12, 48–50). Later studies using molecular genotyping methods revealed no association of *ATM* mutations and early onset of mammary gland cancer (14, 19, 21, 22). However, recent evidence analyzing seven different mutations suggests that ATM mutations in individuals with hereditary mammary gland and ovarian cancers may increase the risk of breast cancer (24). There is, however, no evidence reported previously that suggests that a null mutation in *Atm* may confer any developmental or tumorigenic phenotype.

Our study strongly suggests that the heterozygous loss of *Atm* in the context of *Brca1*-deficient mammary tissue affects the tumor type and invasiveness. In 20 *Atm*$^{+/-}$;*Brca1*-MG-Δex11 mice that developed tumors, all developed invasive, anaplastic carcinomas that displayed atypical mammary architecture, invaded blood vessels, and completely displaced the mammary fat pad after infiltration. In the 24 *Atm*$^{+/+}$;*Brca1*-MG-Δex11 mice, 13 resulting tumors were of the same anaplastic, invasive type as the *Atm*$^{+/-}$;*Brca1*-MG-Δex11 mice. The other 11 tumors, however, were variable in histologic appearance a phenotype reported previously for mammary tumors in *Brca1*-null mice (40). None of the nonanaplastic tumors were found to invade the bloodstream. Although several of the *Atm*$^{+/-}$;*Brca1*-MG-Δex11 tumors were found to penetrate blood vessels, no metastases were discovered. This may be because animals were sacrificed at a tumor burden of ~1 cm, which was reached only a few days after initial detection by palpation. This may not allow sufficient time for a distant tumor to develop to the point of detectability. Of interest, in the control

group (*Atm*$^{+/-}$;*Brca1*$^{Co/Co}$;*MMTV-Cre*−), two tumors formed, both of these tumors were adenocarcinomas, suggesting that our mixed strain background may be predisposed to cancer due to *Atm* haploinsufficiency. The low number of tumors and the design of our study do not allow us to make a definitive conclusion.

Of all 49 tumors, none were found to have metastasized to secondary tissues. This was surprising considering that cells from anaplastic tumors often invaded blood vessels. A previous study reported metastasis in only 3 of 56 *Brca1*$^{Co/Co}$;*MMTV-Cre*+;*p53*$^{-/-}$ mice, suggesting low probability of metastasis due to *Brca1* mutations in the mouse model (40). It is possible that cells were able to establish in secondary tissues but not able to proliferate in those microenvironments. This phenomenon has been observed in other studies using human metastatic mammary gland cancer cells that were inoculated into mouse mammary glands. The cells were found in secondary tissues and able to grow again in culture but not able to proliferate in the secondary tissues (51). Finally, as noted above, mice were sacrificed when tumor burden reached 1 to 2 cm in diameter, so it is also possible that the mice were sacrificed before there was sufficient time for metastasis to occur.

We analyzed chromosome rearrangements, amplifications, and deletions in the *Atm*$^{+/-}$;*Brca1*-MG-Δex11 tumors to determine if haploinsufficiency of *Atm* exacerbated the genomic instability phenotype seen in *Brca1* tumors. Spectral karyotyping and CGH analysis revealed that there were high levels of genomic aberrations in both *Atm*$^{+/-}$;*Brca1*-MG-Δex11 and *Atm*$^{+/+}$;*Brca1*-MG-Δex11 tumors (Fig. 4). There were no significant differences in the average number of chromosome breaks per chromosome between the two genotypes of tumor (Fig. 4*B*). Global analysis of copy number changes suggests gross dysregulation of chromosomal stability (Fig. 4*C*). The degree of chromosomal instability appears to be similar regardless of genotype, aside from the two regions of chromosome 4 and the X chromosome. It is possible that any differences in chromosomal integrity resulting from *Atm* heterozygosity may be masked by the high levels of genomic instability that occur in *Brca1* mutant cells. This may make it impossible to detect the subtle differences between the tumor types. The data obtained correlate with findings reported previously in *Brca1*-MG-Δex11 mice (41) with few differences. In the four tumors analyzed in the current study, we could not detect loss of the proximal region of chromosome 11 where *TRP53* maps, in addition to the deletion of distal chromosome 14 containing the *Rb1* locus. Intriguingly, the amplification on chromosome 11 maps to bands E1 to E2 also in the current study, suggesting that the amplicon might be the result of a high copy number amplification of a novel oncogene (*Spet9*) that we found as being amplified in a variety of mouse models for breast cancer, including BRCA1-associated tumors (52).

Microarray analysis showed that, as expected, noninvasive and invasive tumors displayed different patterns of gene expression, reflecting their obvious histologic differences and state of differentiation. By contrast, *Atm* haploinsufficiency did not detectably affect global gene expression once tumorigenesis has been initiated. Two different methods of analysis were used. We found that only 16 genes were differentially expressed by RMA and 13 by dChip in anaplastic tumors of *Atm* wild-type and heterozygotes. Importantly, only 5 were considered significant by both types of analysis. These findings suggest that the major variable in gene expression is the tumor type, not the tumor genotype. We thought that differences in expression might be found in regions where there were differences in copy number by CGH (Fig. 4*C*). Interestingly, though, none of the differentially expressed genes

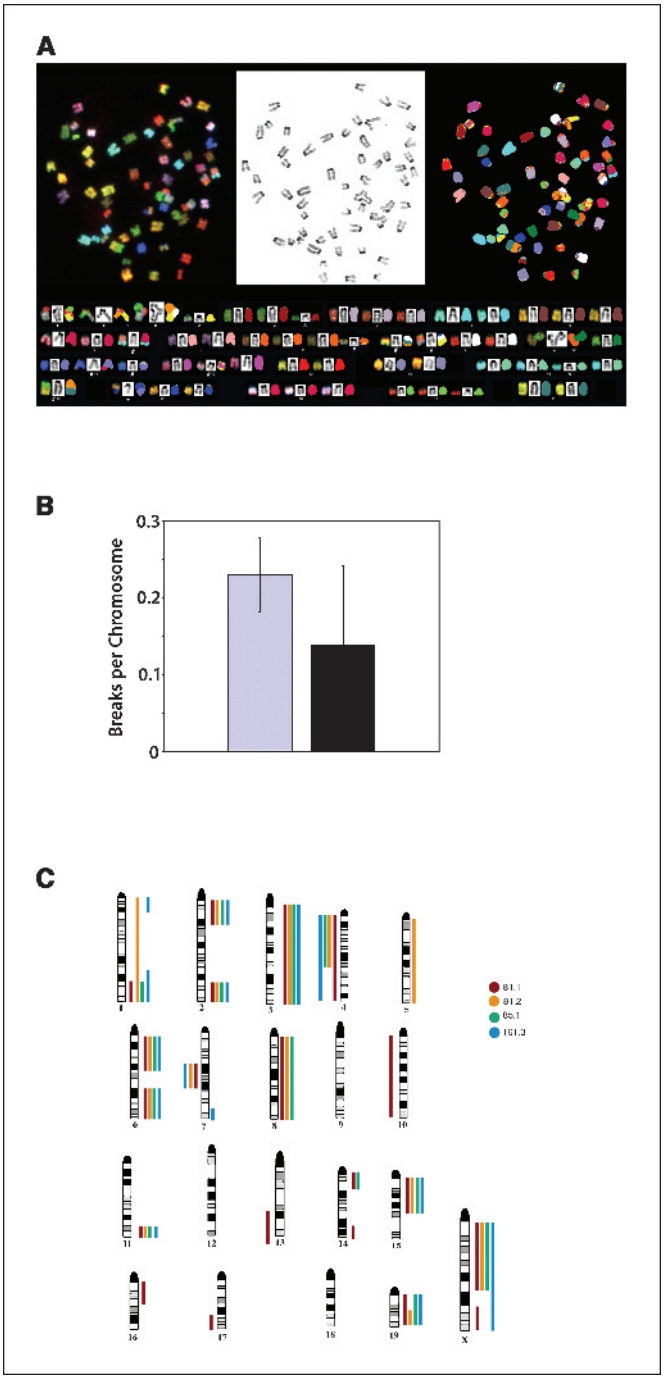

Figure 4. Spectral karyotyping and CGH analysis of tumor chromosomal spreads. *A,* spectral karyotyping revealed high levels of chromosomal aberrations, including complex rearrangements (chromosomes 1, 10, 17), translocations (chromosomes 6, 8, 9(2), 11(2), 12, 16), deletions (chromosomes 1, 2, 15), and duplications (chromosomes 2, 3, 5, 6, 8, 9, 11, 12, 15, 17, 18, 19). There were no recurrent rearrangements seen in any of the tumors analyzed. *B,* numbers of chromosome breakpoints were compared between samples. A total of 890 chromosomes were analyzed in two samples from the *Atm*$^{+/+}$;*Brca1*-MG-Δex11 genotype (*gray*) and 988 chromosomes were analyzed for two *Atm*$^{+/-}$;*Brca1*-MG-Δex11 samples (*black*). The total numbers of breaks detected per chromosome are represented. *C,* map of genomic imbalances derived by CGH. All chromosomes were affected in at least one sample, except chromosomes 9, 12, and 18. A loss of the distal region of chromosome 4 occurred for both *Atm*$^{+/+}$;*Brca1*-MG-Δex11 samples (purple 81.1, blue 161.3) but neither of the *Atm*$^{+/-}$;*Brca1*-MG-Δex11 samples (yellow 81.2, green 85.1). In addition, amplification of the distal end of the X chromosome occurred in the *Atm*$^{+/+}$;*Brca1*-MG-Δex11 samples but not in the *Atm*$^{+/-}$;*Brca1*-MG-Δex11 tumors (*arrowheads*).

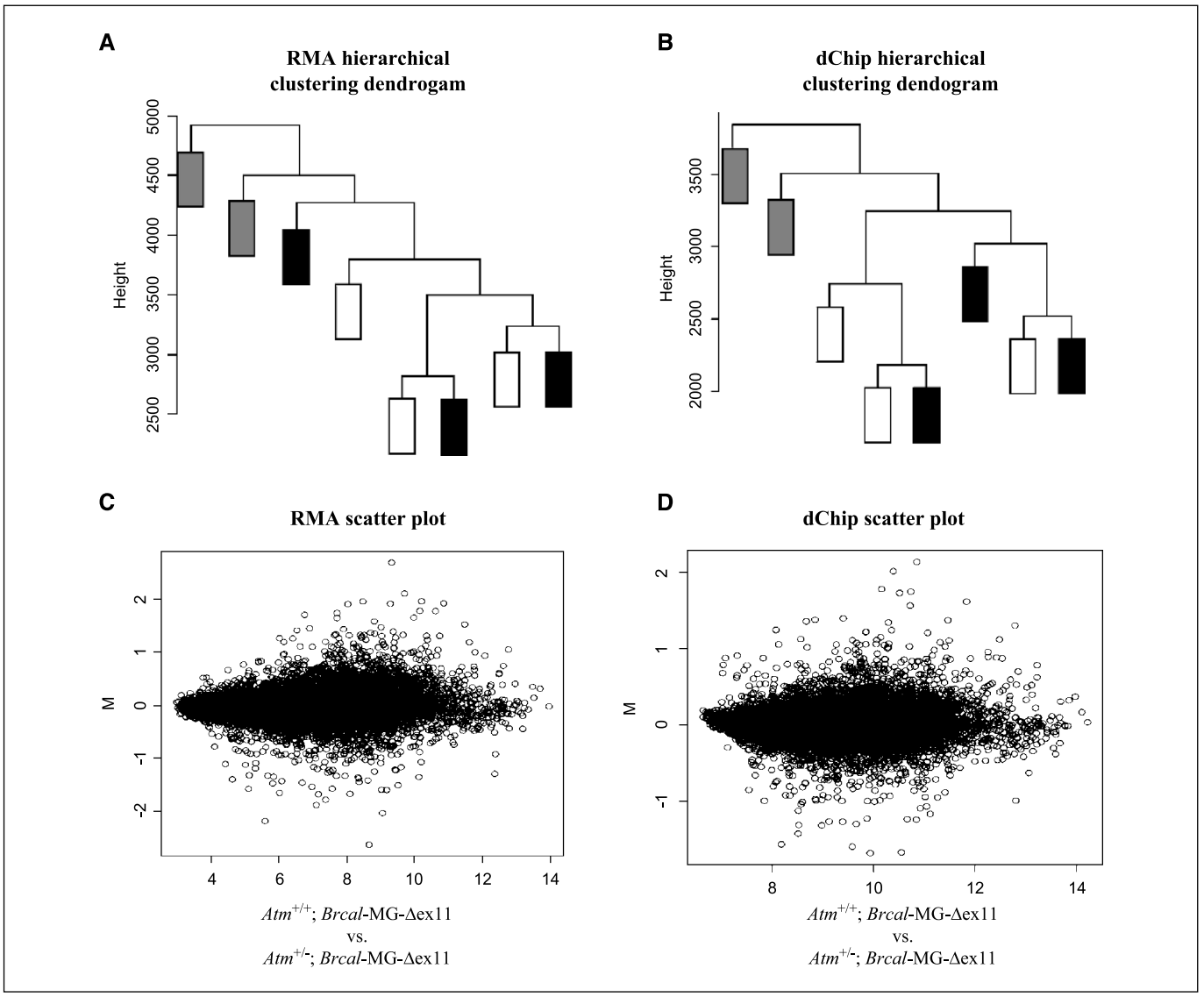

Figure 5. RMA and dChip scatter plot and hierarchical clustering of eight tumor-derived RNA profiles. *A,* hierarchical clustering using RMA indicated that the nonanaplastic tumors (*gray boxes*) clustered the furthest away, whereas the anaplastic tumors seemed to be more similar regardless of genotype (*white boxes, Atm*$^{+/-}$;*Brca1*-MG-Δex11; *black boxes, Atm*$^{+/+}$;*Brca1*-MG-Δex11). *B,* dChip analysis indicated again that the two nonanaplastic tumors were the most different, whereas the anaplastic tumors clustered more closely without respect to genotype (same designations). *C,* RMA scatter plot indicated very few genes differentially expressed between three *Atm*$^{+/-}$;*Brca1*-MG-Δex11 and three *Atm*$^{+/+}$;*Brca1*-MG-Δex11 tumors. *D,* dChip analysis revealed mostly similar expression of genes as well, with a few genes appearing to be differentially expressed.

found in our array analysis correspond to regions on the X chromosome or chromosome 4 where copy number was altered. Although we recognize that our sample size was small, we employed several practical methods to alleviate the statistical issues related to our sample size. First, we obtained gene expression intensities based on two different methods, dChip and RMA, and repeated the analyses using both preprocessing techniques. The purpose of conducting the analyses using two different preprocessing and normalization methods was that genes detected as being differentially expressed between the two types of tumors for both types of analytic methods would have a greater likelihood of being of practical interest. We detected a few genotype differences in anaplastic tumors by two separate methods, supporting a similarity of gene expression based on histologic type and not by genotype. In addition, the clustering dendograms provided a measure for how similarly dChip and RMA classify the data, and in both methods, tumors clustered by histologic type and not by genotype. Thus, our findings indicate that we could differentiate tumors only by histologic type and not by genotype among the anaplastic tumors that are clustered differently between the two methods.

Whole mount analysis revealed that *Brca1*-deficient developing mammary tissue displayed delayed growth and a failure to extend completely into mammary fat tissue during development. Some defects in pregnancy that have been reported previously for *Brca1*-null mammary glands were also noted (35). The *Atm*$^{+/-}$;*Brca1*-MG-Δex11 and *Atm*$^{+/+}$;*Brca1*-MG-Δex11 mice recapitulate these defects, but the *Atm*$^{+/-}$;*Brca1*-MG-Δex11 mice displayed additional subtle developmental abnormalities. The ductal branching during mammary development in virgin females was significantly less than in wild-type and *Brca1*-deficient tissues (Fig. 6*D*). There were no abnormalities of organization of the TEBs, nor were there differences observed in proliferation or apoptosis in these tissues,

suggesting that these differences may be resulting from developmental mechanisms affecting branching but not affecting the rate of proliferation and/or death. The relevance of this phenotype to the increase in anaplastic phenotype is not known, but it may be that certain cells affected by this dysregulation, such as those that are undifferentiated (TEB cap stem cells, for example), could be important during early tumorigenesis. We hypothesize that the branching defects may be related to the developmental defects by influencing the type of cell that becomes tumorigenic, affecting earlier and less differentiated cells in the *Atm/Brca1* double mutant than in the *Brca1* mutant alone.

In summary, our results support the clinical data suggesting that *ATM* heterozygosity may play a role in breast tumorigenesis. *Atm* heterozygosity does not alter the time-dependent development of mammary gland cancers resulting from loss of *Brca1*, but *Atm* haploinsufficiency is able to promote the development of invasive, anaplastic carcinomas in all of the tumors we analyzed. Data from previous clinical studies have identified obligate *ATM* mutant carriers as having an increased risk of certain types of cancer, including hereditary breast cancers (9–18). This implied risk in developing hereditary breast cancer would require primary mutations in other tumor suppressors known to be associated with hereditary breast cancer, such as the *BRCA1* gene. Because ATM directly activates BRCA1 following ionizing radiation, and both BRCA1 and ATM have also been shown to act in response to DNA damage, deficiency of both ATM and BRCA1 may result in increased dysregulation of cell cycle control leading to genomic instability and cancers. Although no differences in chromosomal aberrations and copy number of RNA expression were observed in $Atm^{+/-}$;*Brca1*-MG-Δex11 versus $Atm^{+/+}$;*Brca1*-MG-Δex11 tumors, the severe phenotype of *Brca1* tumors may obscure any uncovered changes due to haploinsufficiency of *Atm*. These observations indicate that the heterozygous loss of *ATM* in addition to the homozygous mutation of *BRCA1* may be of clinical importance.

Atm haploinsufficiency also had an effect on developing mammary glands in virgin female mice. A defect in ductal branching during extension of the mammary ducts into the adipose tissue compared with wild-type and *Brca1* mutant controls was observed. Levels of apoptosis and proliferation were similar in

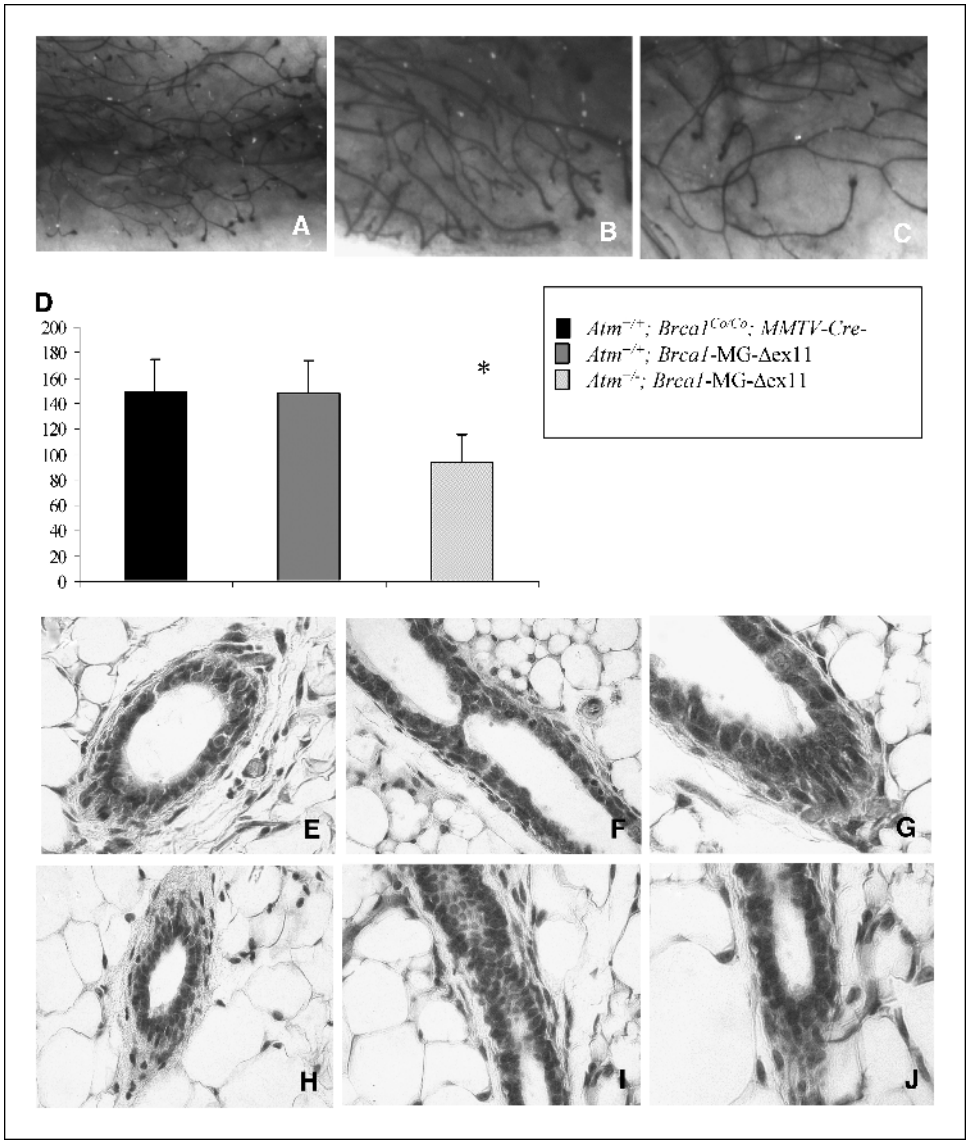

Figure 6. Analysis of abnormalities associated with mammary gland development. *A,* analysis of ductal branching in 7-week-old virgin females from five $Atm^{+/+}$;*Brca1*-MG-Δex11 (*A*), five $Atm^{+/-}$;$Brca1^{Co/Co}$;*MMTV-Cre*− (*B*), and five $Atm^{+/-}$;*Brca1*-MG-Δex11 mice (*C*) revealed that $Atm^{+/-}$;*Brca1*-MG-Δex11 have a decreased amount of ductal bifurcations compared with both controls (*D*). Analysis of ductal morphology revealed that $Atm^{+/-}$;*Brca1*-MG-Δex11 ducts had normally developed ducts on examination of cross-sections (*E*), longitudinal sections (*F*), and TEB morphologies (*G*) compared with $Atm^{+/-}$;$Brca1^{Co/Co}$;*MMTV-Cre*− controls (*H-J*).

Atm$^{+/-}$;*Brca1*-MG-Δex11 versus *Atm*$^{+/-}$;*Brca1*-MG-Δex11, and the morphology of the TEBs appeared normal as well. We offer two potential nonexclusive explanations for our findings. First, it is possible that *Atm* haploinsufficiency affects development (as well as tumorigenesis) by further reducing DNA repair, cell cycle control, and possibly transcriptional regulation than are present in the *Brca1* mutant alone. Because of the similarities in function and because ATM activates BRCA1, it is possible that the additional reduction in ATM protein levels may exacerbate phenotypes associated with mutations in *Brca1* under certain situations, such as hyperproliferation (as in mammary duct elongation) or tumorigenesis. It is tempting to speculate that in the presence of *Atm* haploinsufficiency ATM fails to activate alternative pathways that otherwise compensate for the lack of *Brca1*. The phenotypes associated with absence of functional *Brca1*, such as mammary developmental defects and tumorigenesis, could then be exacerbated when *Atm*, which has similar and somewhat redundant functions with *Brca1*, is reduced in its absence.

Second, *Atm* haploinsufficiency may impair an important damage response mechanism early during the onset of tumorigenesis. Recent reports suggest that tumorigenic events occurring early in cancer progression activate the ATM-regulated checkpoint through deregulation of DNA replication and DNA damage, creating a barrier against tumor progression (53). Further progression of these tumors may rely on the disruption of the DNA damage response components, such as ATM. *Atm* haploinsufficiency may partially repress this response, leading to the occurrence of more invasive tumors.

Although we do not know the precise mechanism of action, our study provides clear evidence that the disruption of *Atm* affects both mammary development and tumorigenesis in a *Brca1* mutant background, suggesting a synergistic interaction in tumorigenesis when both proteins are depleted. In addition, this work corroborates other recent findings suggesting that the disruption of DNA repair machinery early during tumorigenesis may be critical in the progression to cancer (53).

Acknowledgments

Received 5/11/2005; revised 7/21/2005; accepted 7/27/2005.

The costs of publication of this article were defrayed in part by the payment of page charges. This article must therefore be hereby marked *advertisement* in accordance with 18 U.S.C. Section 1734 solely to indicate this fact.

References

1. Easton DF, Bishop DT, Ford D, Crockford GP. Genetic linkage analysis in familial breast and ovarian cancer: results from 214 families. The Breast Cancer Linkage Consortium. Am J Hum Genet 1993;52:678–701.

2. Lavin MF, Shiloh Y. The genetic defect in ataxia-telangiectasia. Annu Rev Immunol 1997;15:177–202.

3. Rotman G, Shiloh Y. ATM: a mediator of multiple responses to genotoxic stress. Oncogene 1999;18:6135–44.

4. Cortez D, Wang Y, Qin J, Elledge SJ. Requirement of ATM-dependent phosphorylation of brca1 in the DNA damage response to double-strand breaks. Science 1999; 286:1162–6.

5. Gatei M, Scott SP, Filippovitch I, et al. Role for ATM in DNA damage-induced phosphorylation of BRCA1. Cancer Res 2000;60:3299–304.

6. Larson JS, Tonkinson JL, Lai MT. A BRCA1 mutant alters G_2-M cell cycle control in human mammary epithelial cells. Cancer Res 1997;57:3351–5.

7. Gowen LC, Avrutskaya AV, Latour AM, Koller BH, Leadon SA. BRCA1 required for transcription-coupled repair of oxidative DNA damage. Science 1998;281: 1009–12.

8. Moynahan ME, Chiu JW, Koller BH, Jasin M. Brca1 controls homology-directed DNA repair. Mol Cell 1999;4: 511–8.

9. Feng J, Yan J, Chen J, et al. Absence of somatic ATM missense mutations in 58 mammary carcinomas. Cancer Genet Cytogenet 2003;145:179–12.

10. Swift M, Morrell D, Massey RB, Chase CL. Incidence of cancer in 161 families affected by ataxia-telangiectasia. N Engl J Med 1991;325:1831–6.

11. Easton DF. Cancer risks in A-T heterozygotes. Int J Radiat Biol 1994;66:S177–82.

12. Athma P, Rappaport R, Swift M. Molecular genotyping shows that ataxia-telangiectasia heterozygotes are predisposed to breast cancer. Cancer Genet Cytogenet 1996;92:130–4.

13. Stankovic T, Kidd AM, Sutcliffe A, et al. ATM mutations and phenotypes in ataxia-telangiectasia families in the British Isles: expression of mutant ATM and the risk of leukemia, lymphoma, and breast cancer. Am J Hum Genet 1998;62:334–45.

14. FitzGerald MG, Bean JM, Hegde SR, et al. Heterozygous ATM mutations do not contribute to early onset of breast cancer. Nat Genet 1997;15:307–10.

15. Chen J, Birkholtz GG, Lindblom P, Rubio C, Lindblom A. The role of ataxia-telangiectasia heterozygotes in familial breast cancer. Cancer Res 1998;58:1376–9.

16. Janin N, Andrieu N, Ossian K, et al. Breast cancer risk in ataxia telangiectasia (AT) heterozygotes: haplotype study in French AT families. Br J Cancer 1999;80:1042–5.

17. Geoffroy-Perez B, Janin N, Ossian K, et al. Cancer risk in heterozygotes for ataxia-telangiectasia. Int J Cancer 2001;93:288–93.

18. Angele S, Hall J. The ATM gene and breast cancer: is it really a risk factor? Mutat Res 2000;462:167–78.

19. Bebb DG, Yu Z, Chen J, et al. Absence of mutations in the ATM gene in forty-seven cases of sporadic breast cancer. Br J Cancer 1999;80:1979–81.

20. Broeks A, Urbanus JH, Floore AN, et al. ATM-heterozygous germline mutations contribute to breast cancer-susceptibility. Am J Hum Genet 2000;66:494–500.

21. Izatt L, Greenman J, Hodgson S, et al. Identification of germline missense mutations and rare allelic variants in the ATM gene in early-onset breast cancer. Genes Chromosomes Cancer 1999;26:286–94.

22. Vorechovsky I, Rasio D, Luo L, et al. The ATM gene and susceptibility to breast cancer: analysis of 38 breast tumors reveals no evidence for mutation. Cancer Res 1996;56:2726–32.

23. Chenevix-Trench G, Spurdle AB, Gatei M, et al. Dominant negative ATM mutations in breast cancer families. J Natl Cancer Inst 2002;94:205–15.

24. Thorstenson YR, Roxas A, Kroiss R, et al. Contributions of ATM mutations to familial breast and ovarian cancer. Cancer Res 2003;63:3325–33.

25. Szabo CI, Schutte M, Broeks A, et al. Are ATM mutations 7271T->G and IVS10-6T->G really high-risk breast cancer-susceptibility alleles? Cancer Res 2004;64: 840–3.

26. Waha A, Sturne C, Kessler A, et al. Expression of the ATM gene is significantly reduced in sporadic breast carcinomas. Int J Cancer 1998;78:306–9.

27. Kairouz R, Clarke RA, Marr PJ, et al. ATM protein synthesis patterns in sporadic breast cancer. Mol Pathol 1999;52:252–6.

28. Spring K, Ahangari F, Scott SP, et al. Mice heterozygous for mutation in Atm, the gene involved in ataxia-telangiectasia, have heightened susceptibility to cancer. Nat Genet 2002;32:185–90.

29. Gowen LC, Johnson BL, Latour AM, Sulik KK, Koller BH. Brca1 deficiency results in early embryonic lethality characterized by neuroepithelial abnormalities. Nat Genet 1996;12:191–4.

30. Liu CY, Flesken-Nikitin A, Li S, Zeng Y, Lee WH. Inactivation of the mouse Brca1 gene leads to failure in the morphogenesis of the egg cylinder in early postimplantation development. Genes Dev 1996;10: 1835–43.

31. Hakem R, de la Pompa JL, Sirard C, et al. The tumor suppressor gene Brca1 is required for embryonic cellular proliferation in the mouse. Cell 1996;85:1009–23.

32. Ludwig T, Chapman DL, Papaioannou VE, Efstratiadis A. Targeted mutations of breast cancer susceptibility gene homologs in mice: lethal phenotypes of Brca1, Brca2, Brca1/Brca2, Brca1/p53, and Brca2/p53 nullizygous embryos. Genes Dev 1997;11: 1226–41.

33. Shen SX, Weaver Z, Xu X, et al. A targeted disruption of the murine Brca1 gene causes γ-irradiation hypersensitivity and genetic instability. Oncogene 1998;17: 3115–24.

34. Xu X, Weaver Z, Linke SP, et al. Centrosome amplification and a defective G_2-M cell cycle checkpoint induce genetic instability in BRCA1 exon 11 isoform-deficient cells. Mol Cell 1999;3:389–95.

35. Xu X, Wagner KU, Larson D, et al. Conditional mutation of Brca1 in mammary epithelial cells results in blunted ductal morphogenesis and tumour formation. Nat Genet 1999;22:37–43.

36. Hemminki K, Granstrom C. Morphological types of breast cancer in family members and multiple primary tumours: is morphology genetically determined? Breast Cancer Res 2002;4:R7.

37. Russo J, Russo IH. Cellular basis of breast cancer susceptibility. Oncol Res 1999;11:169–78.

38. Barlow C, Hirotsune S, Paylor R, et al. Atm-deficient mice: a paradigm of ataxia telangiectasia. Cell 1996;86: 159–71.

39. Liyanage M, Weaver Z, Barlow C, et al. Abnormal rearrangement within the α/δ T-cell receptor locus in lymphomas from Atm-deficient mice. Blood 2000;96: 1940–6.

40. Brodie SG, Xu X, Qiao W, et al. Multiple genetic changes are associated with mammary tumorigenesis in Brca1 conditional knockout mice. Oncogene 2001;20: 7514–23.

41. Weaver Z, Montagna C, Xu X, et al. Mammary tumors in mice conditionally mutant for Brca1 exhibit gross

genomic instability and centrosome amplification yet display a recurring distribution of genomic imbalances that is similar to human breast cancer. Oncogene 2002; 21:5097–107.
42. Wagner KU, Wall RJ, St-Onge L, et al. Cre-mediated gene deletion in the mammary gland. Nucleic Acids Res 1997;25:4323–30.
43. Wagner KU, McAllister K, Ward T, et al. Spatial and temporal expression of the Cre gene under the control of the MMTV-LTR in different lines of transgenic mice. Transgenic Res 2001;10:545–53.
44. Guy CT, Cardiff RD, Muller WJ. Induction of mammary tumors by expression of polyomavirus middle T oncogene: a transgenic mouse model for metastatic disease. Mol Cell Biol 1992;12:954–61.
45. Deng CX, Brodie SG. Roles of BRCA1 and its interacting proteins. Bioessays 2000;22:728–37.
46. Wang Q, Zhang H, Fishel R, Greene MI. BRCA1 and cell signaling. Oncogene 2000;19:6152–8.
47. Sorlie T, Tibshirani R, Parker J, et al. Repeated observation of breast tumor subtypes in independent gene expression data sets. Proc Natl Acad Sci U S A 2003;100:8418–23.
48. Olsen JH, Hahnemann JM, Borresen-Dale AL, et al. Cancer in patients with ataxia-telangiectasia and in their relatives in the Nordic countries. J Natl Cancer Inst 2001;93:121–7.
49. Swift M, Reitnauer PJ, Morrell D, Chase CL. Breast and other cancers in families with ataxia-telangiectasia. N Engl J Med 1987;316:1289–94.
50. Swift M, Sholman L, Perry M, Chase C. Malignant neoplasms in the families of patients with ataxia-telangiectasia. Cancer Res 1976;36:209–15.
51. Goodison S, Kawai K, Hihara J, et al. Prolonged dormancy and site-specific growth potential of cancer cells spontaneously disseminated from nonmetastatic breast tumors as revealed by labeling with green fluorescent protein. Clin Cancer Res 2003;9:3808–14.
52. Montagna C, Lyu MS, Hunter K, et al. The Septin 9 (MSF) gene is amplified and overexpressed in mouse mammary gland adenocarcinomas and human breast cancer cell lines. Cancer Res 2003;63:2179–87.
53. Bartkova J, Horejsi Z, Koed K, et al. DNA damage response as a candidate anti-cancer barrier in early human tumorigenesis. Nature 2005;434:864–70.